inorganics

MDPI

Article

Supramolecular Structure and Antimicrobial Activity of Ni(II) Complexes with s-Triazine/Hydrazine Type Ligand

Eman M. Fathalla [1,*], Morsy A. M. Abu-Youssef [1,*], Mona M. Sharaf [2], Ayman El-Faham [1], Assem Barakat [3], Matti Haukka [4] and Saied M. Soliman [1,*]

[1] Department of Chemistry, Faculty of Science, Alexandria University, P.O. Box 426, Ibrahimia, Alexandria 21321, Egypt; ayman.elfaham@alexu.edu.eg or aymanel_faham@hotmail.com
[2] Protein Research Department, Genetic Engineering and Biotechnology Research Institute, City of Scientific Research and Technological Applications, Alexandria P.O. Box 21933, Egypt; sharafmona4@gmail.com
[3] Department of Chemistry, College of Science, King Saud University, P.O. Box 2455, Riyadh 11451, Saudi Arabia; ambarakat@ksu.edu.sa
[4] Department of Chemistry, University of Jyväskylä, P.O. Box 35, FI-40014 Jyväskylä, Finland; matti.o.haukka@jyu.fi
* Correspondence: eman.nomeir@alexu.edu.eg (E.M.F.); morsy5@alexu.edu.eg (M.A.M.A.-Y.); saied1soliman@yahoo.com or saeed.soliman@alexu.edu.eg (S.M.S.)

Abstract: The two complexes, $[Ni(DPPT)_2](NO_3)_2{*}1.5H_2O$ (**1**) and $[Ni(DPPT)(NO_3)Cl].EtOH$ (**2**), were synthesized using the self-assembly of (*E*)-2,4-di(piperidin-1-yl)-6-(2-(1-(pyridin-2-yl)ethylidene)hydrazinyl)-1,3,5-triazine (**DPPT**) with $Ni(NO_3)_2{*}6H_2O$ in the absence and presence of $NiCl_2{*}6H_2O$, respectively. In both cases, the neutral tridentate **DPPT** ligand is found coordinated to the Ni(II) via three N-atoms from the hydrazone, pyridine and *s*-triazine rings. Hence, the homoleptic complex **1** has a NiN_6 hexa-coordination environment while two NO_3^- are counter anions in addition to one-and-a-half crystallized hydration water molecules are found acting as an outer sphere. The heteroleptic complex **2** has a NiN_3O_2Cl coordination sphere where the coordination environment of the Ni(II) is completed by one bidentate nitrate and one chloride ion leading to a neutral inner sphere while the outer sphere contains one crystallized ethanol molecule. Both complexes have distorted octahedral coordination environments around the Ni(II) ion. Using Hirshfeld analysis, the intermolecular contacts H . . . H and O . . . H in **1** and the Cl . . . H, O . . . H, N . . . H, H . . . H, C . . . H and C . . . C in **2** are found to be the most important for crystal stability. The antimicrobial activity of complexes **1** and **2** was assessed against different bacterial and fungal strains, and the results were compared with the free ligand as well as the antibacterial (*Gentamycin*) and antifungal (Ketoconazole) positive controls. Both Ni(II) complexes are better antibacterial and antifungal agents than the free ligand. Interestingly, both Ni(II) complexes have similar antifungal activity against *C. albicans* compared to Ketoconazole.

Keywords: Ni(II); *s*-triazine; Schiff base; Hirshfeld; antibacterial; antifungal

Citation: Fathalla, E.M.; Abu-Youssef, M.A.M.; Sharaf, M.M.; El-Faham, A.; Barakat, A.; Haukka, M.; Soliman, S.M. Supramolecular Structure and Antimicrobial Activity of Ni(II) Complexes with s-Triazine/Hydrazine Type Ligand. *Inorganics* **2023**, *11*, 253. https://doi.org/10.3390/inorganics11060253

Academic Editors: Wolfgang Linert, Gabriel García Sánchez, David Turner and Koichiro Takao

Received: 22 May 2023
Revised: 1 June 2023
Accepted: 7 June 2023
Published: 9 June 2023

1. Introduction

Increased mortality by pathogenic diseases due to antimicrobial resistance (AMR) has become a serious hazard to human health and economic progress. The World Health Organization (WHO) has listed AMR among the top 10 worldwide public health challenges to humanity [1,2]. For this concern, medicinal inorganic chemistry is crucial for the development of new drugs [3–5]. Because of the important roles of transition metal ions and their complexes in biological processes due to their ability to treat a variety of diseases, chemists are investigating these compounds to enhance their pharmacological activities. Numerous studies on antibacterial agents have shown that the potency of the ligand is increased if it is chelated with a metal ion [6–8]. The Overtone concept and Tweedy's chelation theory were used to present a potential mechanism for the higher activity of

metal chelates [9]. Additionally, chelation could make the core metal more lipophilic to facilitate its penetration across the lipid bilayers of the cell membrane, which would boost the uptake of the metal chelates [10].

Additionally, most 3D-block elements and their coordination compounds have a biological necessity and a diversity of acknowledged bioactivities. Urease is a well-identified nickel enzyme that drives researchers to further investigate the coordination chemistry of Ni(II) complexes [11,12]. These Ni(II) complexes have the ability to permeate the microbial membrane and affect the enzyme activity leading to wide-spectrum action against microbes [13–19].

On the other hand, nitrogen heterocycles are included in around 75% of small-molecule medicines [20]. This can be attributed to the capacity of the nitrogen atom to quickly form hydrogen bonds with biological targets [21–23]. Among these important nitrogen heterocycles, hydrazone Schiff bases have attracted the interest of researchers due to their chelating diversity as a result of their well-known structural flexibility [24–28]. In addition, hydrazones enhance cytotoxicity, which could help in constructing promising anticancer agents [29]. Furthermore, *s*-triazine-hydrazino derivatives have received considerable attention [30–32], with a special interest in coordination and supramolecular chemistry [33,34], as well as their enormous potential in medicines [35].

In our previous work, we reported the synthesis and antimicrobial activity of the Cu(II), Mn(II) and Ni(II) complexes with the *s*-triazine/hydrazine type ligand, namely, 2,4-*bis*(morpholin-4-yl)-6-[(*E*)-2-[1-(pyridin-2-yl)ethylidene]hydrazin-1-yl]-1,3,5-triazine, (**DMPT**) [36,37]. To continue this work, the present study aims to synthesize two nitrogen-containing Ni(II) complexes using the *s*-triazine ligand **DPPT** shown in Figure 1. The supramolecular structure of the synthesized complexes has been explored based on single-crystal X-ray diffraction (SCXRD) and Hirshfeld calculations. Additionally, the antimicrobial activity of the Ni(II) complexes against six harmful microorganisms was assessed.

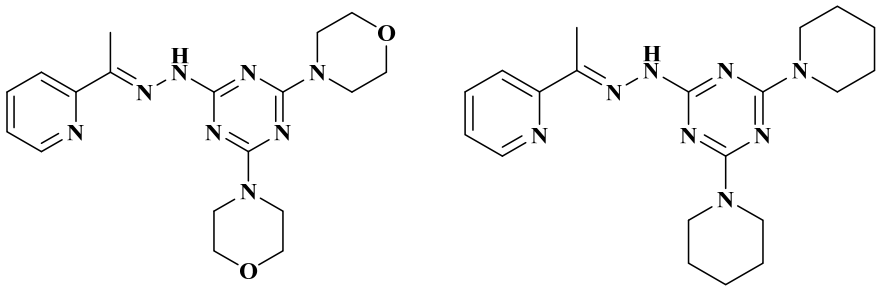

Figure 1. Structure of (*E*)-2,4-di(piperidin-1-yl)-6-(2-(1-(pyridin-2-yl)ethylidene) hydrazinyl)-1,3,5-triazine (**DPPT**) and its previously published analogue (**DMPT**) [36,37].

2. Results and Discussion

2.1. Synthesis and Characterizations

The organic ligand (**DPPT**) was synthesized by a reaction of 2-hydrazinyl-4,6-di(piperidin-1-yl)-1,3,5-triazine with 2-acetylpyridine in ethanol by heating under reflux conditions. The target hydrazone was obtained in high yield and with high purity and then used as it is for the preparation of the two Ni(II) complexes, as shown in Scheme 1. The Ni(II) complexes were obtained in a highly crystalline form via self-assembly of **DPPT** and $Ni(NO_3)_2$*$6H_2O$ in ethanol in the absence and presence of $NiCl_2$*$6H_2O$ affording the monomeric complexes $[Ni(DPPT)_2](NO_3)_2$*$1.5H_2O$ (**1**) and $[Ni(DPPT)(NO_3)Cl]$.EtOH (**2**), respectively, as shown in Scheme 1. Both complexes were air stable for a long time, and the crystal quality was not changed over time. Additionally, complexes **1** and **2** are soluble in polar protic solvents such as ethanol and methanol, as well as in polar aprotic solvents such as DMSO, DMF and acetonitrile. Their structures were confirmed using single-crystal X-ray crystallography (SCXRD).

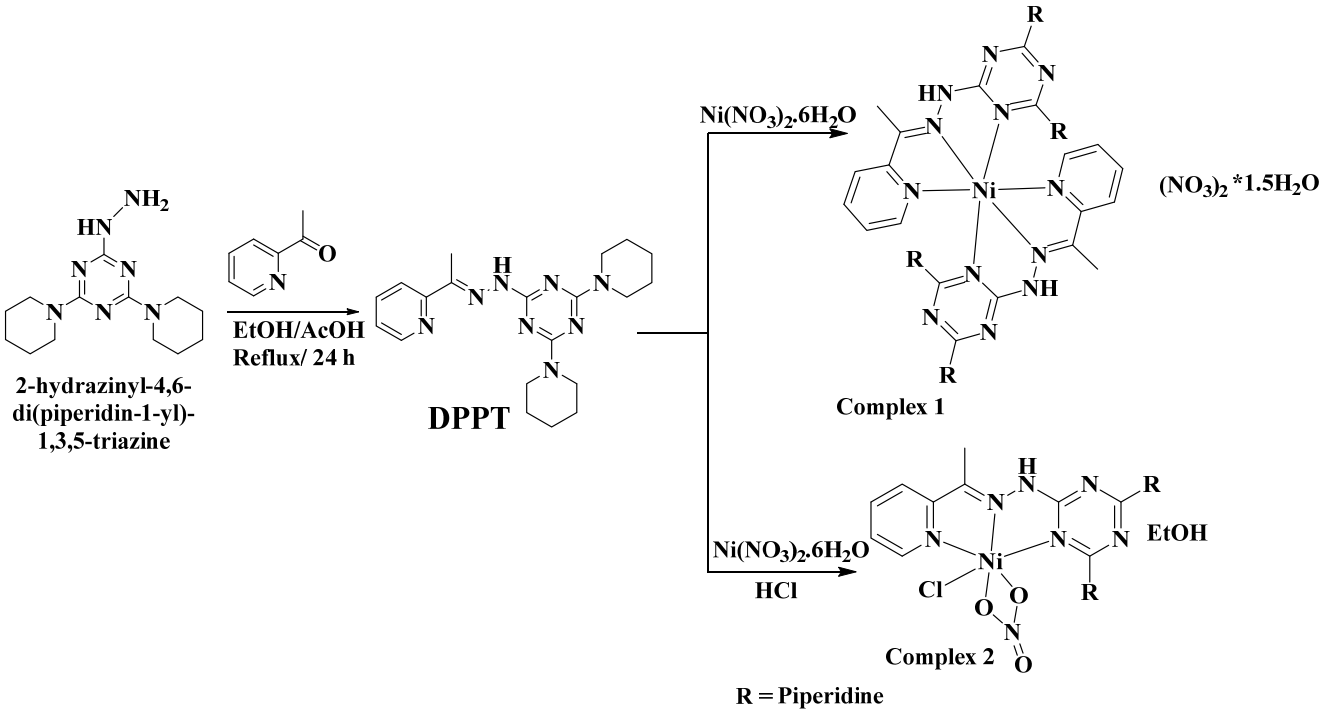

Scheme 1. Synthesis of the ligand **DPPT** and their Ni(II) complexes **1** and **2**.

2.2. X-ray Structure

2.2.1. X-ray Structure of **1**

The structure of the homoleptic complex, $[Ni(DPPT)_2](NO_3)_2{*}1.5H_2O$ (**1**), was confirmed using single-crystal X-ray diffraction. It crystallized in the monoclinic crystal system and *C2/c* as a space group. The asymmetric formula of complex **1** contains half of the formula above. In the unit cell, there are two $[Ni(DPPT)_2](NO_3)_2{*}1.5H_2O$ formulas, and the unit cell volume is 4517.8(2) $Å^3$ while the calculated density is 1.427 Mg/m^3. The presentation of the coordination sphere of complex **1** is shown in Figure 2.

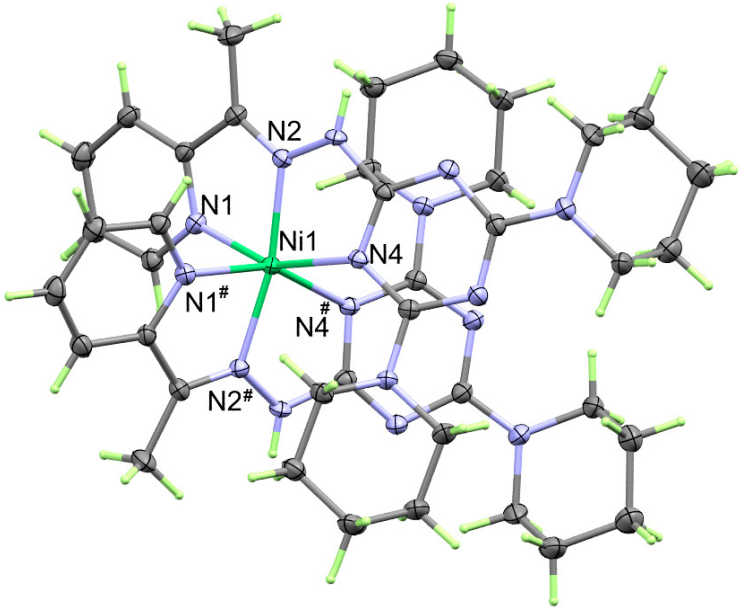

Figure 2. Structure of the coordination sphere of $[Ni(DPPT)_2](NO_3)_2{*}1.5H_2O$ (**1**). The nitrate counter anions and the crystal water were omitted for better clarity. The symmetry code # is −x,y,−z+1/2. The crystal water and the nitrate counter anions were removed from this figure for more clarity.

In complex **1**, the Ni(II) is hexa-coordinated with two **DPPT** ligand units as a neutral tridentate ligand via three N-atoms from the hydrazone, pyridine and *s*-triazine moieties. Hence, the coordination sphere of this complex is the cationic formula $[Ni(DPPT)_2]^{2+}$, while the outer sphere comprises two NO_3^- ions in addition to one-and-a-half crystal water. The respective bond distances and angles are depicted in Table 1. It is clear that the Ni1-N2 bond (2.015(2) Å) with the hydrazone N-atom is the shortest, while the Ni1-N1 (2.087(2) Å) with the pyridine and Ni1-N4 (2.139(2) Å) with the triazine moieties are significantly longer. Due to symmetry consideration, the other three Ni-N bonds with the second **DPPT** ligand unit are symmetry-related and have similar bond distances. The two bite angles of the tridentate chelate are 77.67(9) and 77.27(9)° for N2-Ni1-N1 and N2-Ni1-N4, respectively. The bond angles of the *cis* Ni-N bonds are found in the range of 77.27(9) to 111.45(9)° while the trans N-Ni-N bond angles range from 154.63(9) to 168.65(13)°. Hence, the NiN_6 coordination sphere has a distorted octahedral geometry.

Table 1. The Ni-N distances (Å) and N-Ni-N angles (°) in the $[Ni(DPPT)_2](NO_3)_2$*$1.5H_2O$ complex.

Bond	Distance	Bond	Distance
Ni1-N2	2.015(2)	Ni1-N4	2.139(2)
Ni1-N1	2.087(2)		
Bonds	**Angle**	**Bonds**	**Angle**
N2 $^{\#1}$-Ni1-N2	168.65(13)	N1-Ni1-N4	154.63(9)
N2 $^{\#1}$-Ni1-N1	93.91(9)	N1 $^{\#1}$-Ni1-N4	100.12(9)
N2-Ni1-N1	77.67(9)	N4 $^{\#1}$-Ni1-N4	85.46(12)
N1-Ni1-N1 $^{\#1}$	85.44(13)	N2-Ni1-N4 $^{\#1}$	111.45(9)
N2-Ni1-N4	77.27(9)		

$^{\#1}$ −x,y,−z+1/2.

As clearly seen from Figure 3, the packing view of complex 1 along the crystallographic *a*-direction shows the cationic complex units and the outer sphere of the complex in an alternating manner. The nitrate anion and the crystal water molecule are found in the spaces between these complex cationic units (Figure 3A). The nitrate anion and the crystal water, which represent the polar part of this complex, form a complicated set of C-H . . . O and N-H . . . O interactions with the less polar part $[Ni(DPPT)_2]^{2+}$. A view of the packing scheme along the same direction showing the most important C-H . . . O and N-H . . . O interactions is shown in Figure 3B, while the corresponding hydrogen bond parameters are depicted in Table 2.

Table 2. Hydrogen bond geometric parameters in complex **1**.

D-H . . . A	D-H	H . . . A	D . . . A	D-H . . . A
C7-H7A . . . O3 $^{\#1}$	0.98	2.4	3.292(6)	150.6
N3-H3 . . . O3 $^{\#1}$	0.84(3)	2.05(3)	2.848(5)	158(3)
C1-H1 . . . O4 $^{\#2}$	0.95	2.43	3.261(6)	146.2
C2-H2 . . . O1 $^{\#2}$	0.95	2.45	3.388(6)	171.4
C7-H7B . . . O4 $^{\#3}$	0.98	2.41	3.109(7)	127.9
O4-H4A . . . O3	0.85	1.86	2.665(8)	158.7

$^{\#1}$ $-x,y,-z+\frac{1}{2}$; $^{\#2}$ −x+1/2,−y+1/2,−z+1; $^{\#3}$ x−1/2,−y+1/2,z−1/2.

2.2.2. X-ray Structure of **2**

The structure of the heteroleptic complex **2** was found to be $[Ni(DPPT)(NO_3)Cl].EtOH$, which represents the asymmetric unit of **2** (Figure 4). This complex crystallized in the less symmetric triclinic crystal system and *P-1* space group. In the unit cell, there are two molecules of the asymmetric formula $[Ni(DPPT)(NO_3)Cl].EtOH$ and its volume is 1282.43(4) $Å^3$, while the calculated density is 1.509 Mg/m^3.

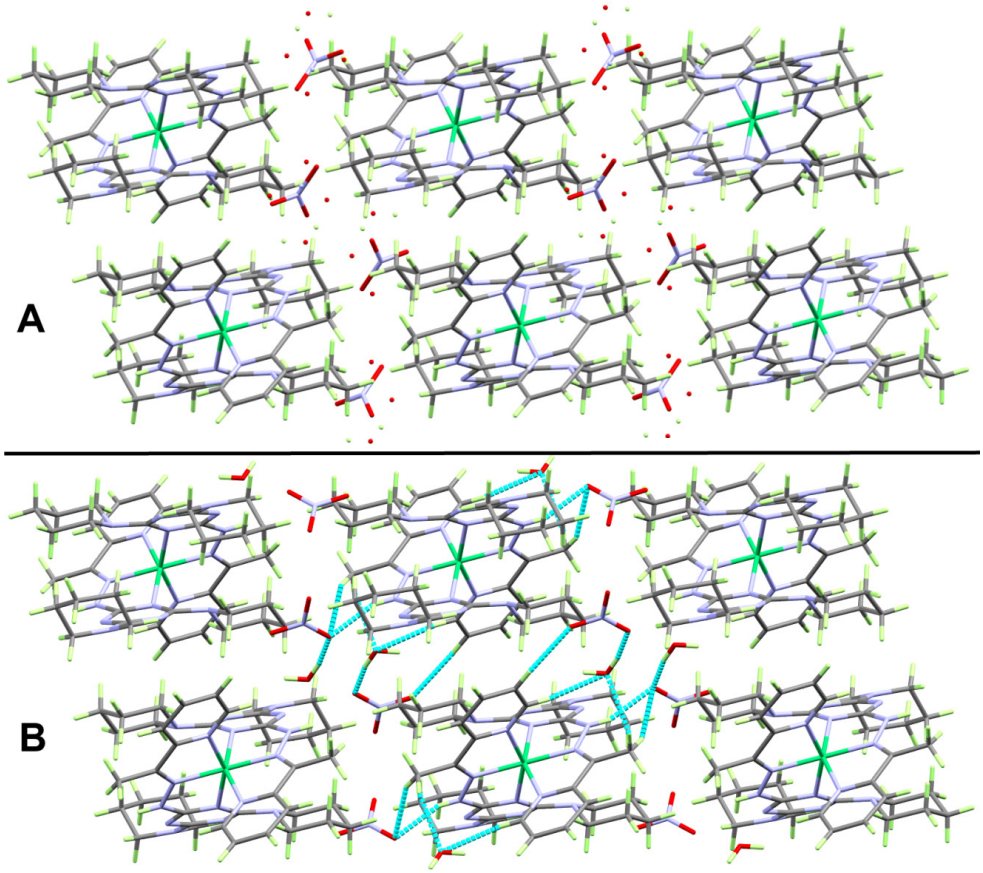

Figure 3. Packing views of complex **1** along *b* directions showing the disordered nitrate counter ion and the crystal water molecule interpenetrating the cationic complex unit (**A**) and connecting the $[Ni(DPPT)_2]^{2+}$ units via C-H . . . O and N-H . . . O (**B**) interactions (Table 2).

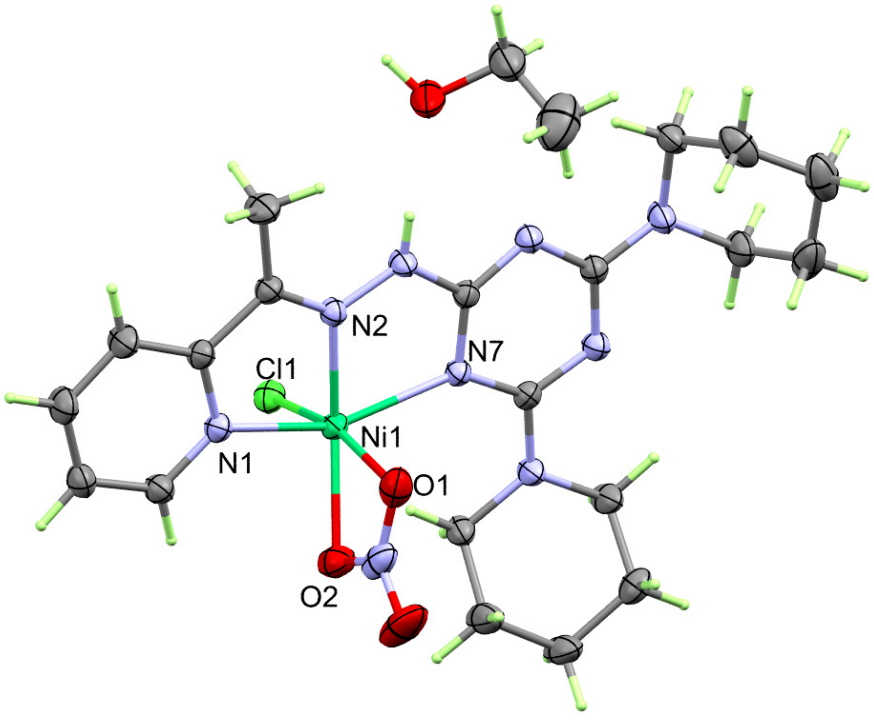

Figure 4. Structure of $[Ni(DPPT)(NO_3)Cl].EtOH$ complex (**2**).

The Ni(II) is coordinated with one tridentate **DPPT** ligand, one bidentate nitrate ion and one monodentate chloride ion. The hexa-coordination sphere of complex **2** is neutral, and hence there is not any counter anion in the outer sphere of this complex. On the other hand, there is one ethanol molecule as a crystal solvent which plays an important role in the molecular packing of this complex. The three Ni-N bonds are not equidistant. The order of the Ni-N bond lengths is $Ni\text{-}N_{(hydrazone)} < Ni\text{-}N_{(pyridine)} < Ni\text{-}N_{(triazine)}$. The corresponding bond distances are 1.9832(14), 2.0765(13) and 2.2249(13) Å, respectively. The bite angles N2-Ni1-N1 and N2-Ni1-N7 are 78.69(5) and 78.23(5)°, respectively, while the N1-Ni1-N7 angle is 156.91(5)°. In complex **2**, there are two short Ni-O interactions with the nitrate ion, which acts as a bidentate ligand via Ni1-O1 and Ni1-O2 bonds. The respective distances are 2.0982(14) and 2.1352(14) Å, while a very small bite angle of 61.09(6)° for the bidentate nitrate was noted. A sixth bond with the coordinated chloride (Ni1-Cl1), which is the longest in the coordination sphere, was also found. As clearly seen from Table 3, all angles deviated significantly from the ideal values for a perfect octahedron (90 and 180°). Hence, the coordination geometry of this complex is a distorted octahedron.

Table 3. Geometric parameters (Å and °) of the coordination environment for [Ni(DPPT)(NO_3)Cl].EtOH complex.

Bond	**Distance**	**Bond**	**Distance**
Ni1-N2	1.9832(14)	Ni1-O1	2.0982(14)
Ni1-N1	2.0765(13)	Ni1-O2	2.1352(14)
Ni1-N7	2.2249(13)	Ni1-Cl1	2.3407(5)
Bonds	**Angle**	**Bonds**	**Angle**
N2-Ni1-N1	78.69(5)	O1-Ni1-N7	90.53(5)
N2-Ni1-O1	96.13(6)	O2-Ni1-N7	112.05(5)
N1-Ni1-O1	92.47(5)	N2-Ni1-Cl1	100.40(4)
N2-Ni1-O2	153.98(6)	N1-Ni1-Cl1	91.64(4)
N1-Ni1-O2	89.29(5)	O1-Ni1-Cl1	163.44(4)
O1-Ni1-O2	61.09(6)	O2-Ni1-Cl1	102.95(4)
N2-Ni1-N7	78.23(5)	N7-Ni1-Cl1	91.96(4)
N1-Ni1-N7	156.91(5)		

The supramolecular structure of this complex is controlled by a number of hydrogen bonding interactions, including the N-H ... O, C-H ... O, C-H ... N and O-H ... Cl interactions listed in Table 4, while the presentation of the most important contacts is shown in Figure 5A. The N3-H3N ... O4 H-bond occurs between the N3-H3 group of the hydrazone moiety as a H-bond donor with an O4 atom of ethanol as a H-bond acceptor. The C7-H7A ... O4 and C7-H7C ... N3 interactions occurred between the C-H bond from the methyl group as a H-bond donor with the O4 and N3 atoms of the OH and NH groups as a H-bond acceptor. In addition, the coordinated chloride participated in the molecular packing via the formation of an O4-H4O ... Cl1 hydrogen bond. These non-covalent interactions connect the complex units leading to the hydrogen-bonded dinuclear formula shown in Figure 5B.

Table 4. Hydrogen bond parameters in [Ni(DPPT)(NO_3)Cl].EtOH.

D-H ... A	**D-H**	**H ... A**	**D ... A**	**D-H ... A**
N3-H3N ... O4	0.82(2)	2.05(2)	2.870(2)	178(2)
C7-H7A ... O4	0.98	2.33	3.166(3)	143.2
C7-H7C ... N3 [#1]	0.98	2.47	3.412(3)	161.1
O4-H4O ... Cl1 [#1]	0.90(3)	2.20(3)	3.1048(17)	174(3)

[#1] −x+1,−y+1,−z+1.

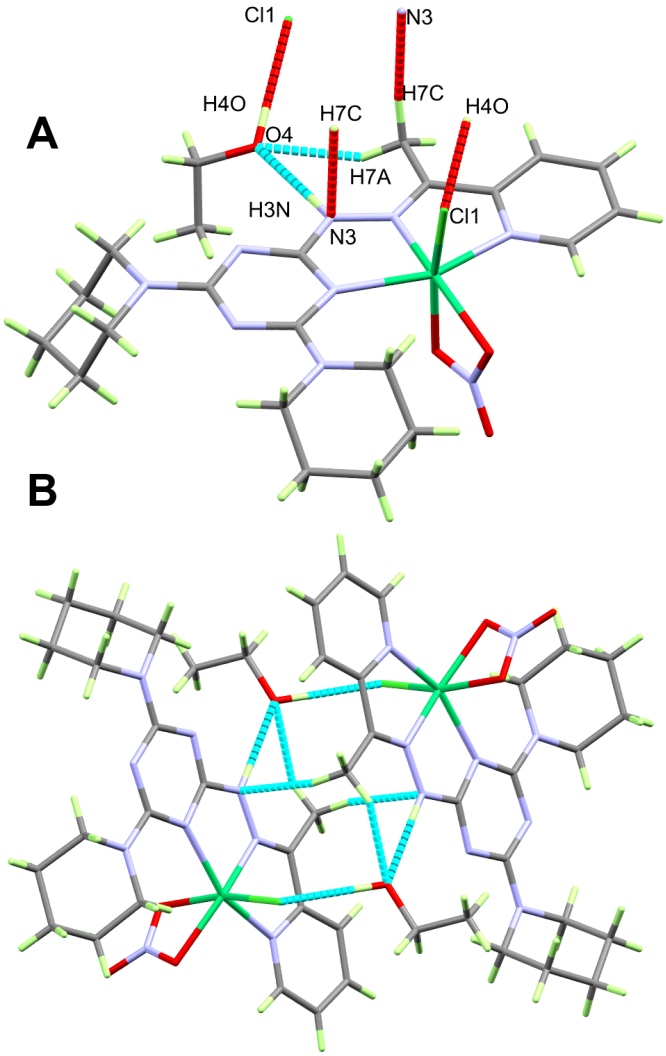

Figure 5. All important hydrogen bond contacts (**A**) and packing scheme (**B**) in [Ni(DPPT)(NO_3)Cl].EtOH complex.

2.3. Hirshfeld Analysis of Molecular Packing

In crystalline materials, the intermolecular interactions play a vital role in the crystal stability. Hirshfeld topology analysis is important for predicting all possible intermolecular contacts in the crystal structure. The d_{norm}, curvedness and shape index surfaces of complex **2** are shown in Figure 6. In the d_{norm} map, the red-colored regions are related to the Cl . . . H, O . . . H, N . . . H, H . . . H, C . . . H and C . . . C intermolecular contacts, which have shorter interaction distances compared to the vdWs radii sum of the interacting atoms. These intermolecular contacts contributed by 8.9, 16.0, 10.2, 52.4, 8.3 and 1.6% from the whole contacts occurred in the crystal structure of complex **2**. A list of the shortest Cl . . . H, O . . . H, N . . . H, H . . . H, C . . . H and C . . . C interactions are given in Table 5.

Table 5. The short intermolecular interactions in **2**.

Contact	Distance	Contact	Distance
Cl1 . . . H4O	2.125	H4 . . . H4	2.044
O4 . . . H7A	2.244	H21B . . . H10A	2.16
O4 . . . H3N	1.861	C15 . . . H12B	2.65
N3 . . . H7C	2.373	C16 . . . O3	3.204
N7 . . . H12B	2.584		

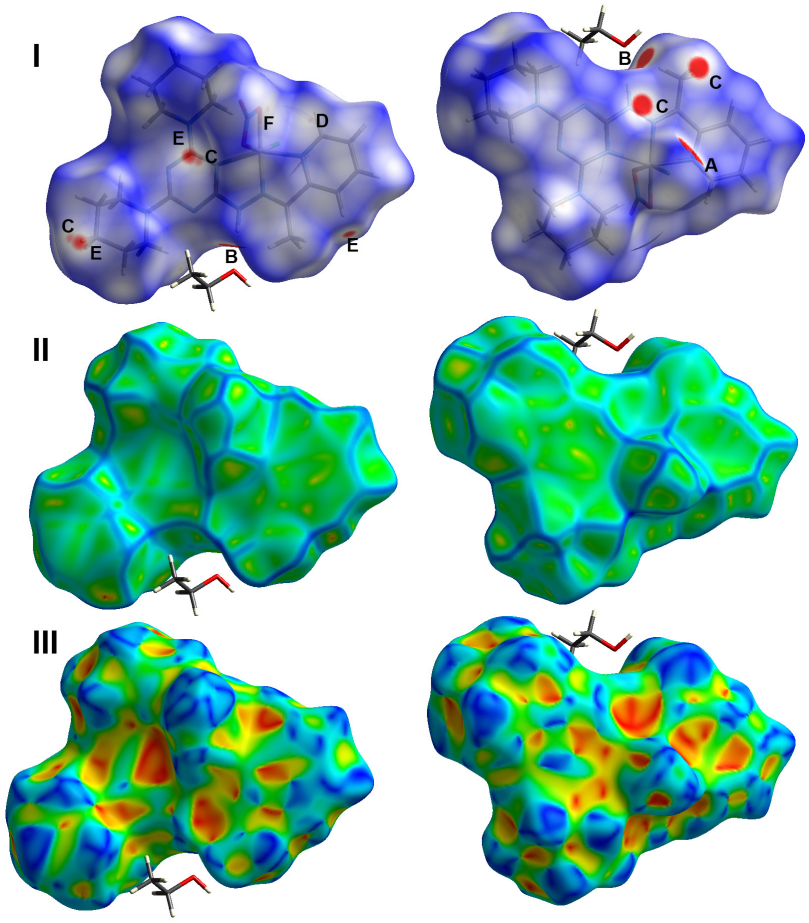

Figure 6. Hirshfeld surfaces: (**I**) d_{norm}, (**II**) curvedness and (**III**) shape index of **2**.

Other contacts are also detected in the crystal structure of this complex but have less significance in the molecular packing as these contacts have long interaction distances. A summary of all contacts contributing to the molecular packing of **2** is presented in Figure 7. Their percentages are depicted in the same illustration.

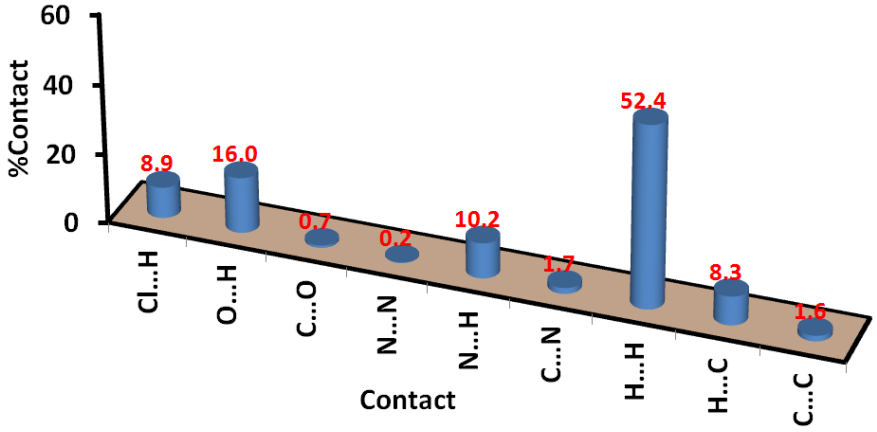

Figure 7. Intermolecular interactions in **2**.

Analysis of the fingerprint plots not only gave a quantitative summary of all possible intermolecular contacts but also shed light on the importance of these interactions on the molecular packing. All Cl ... H, O ... H, N ... H, H ... H, C ... H and C ... C contacts have clear, sharp spikes in the corresponding fingerprint plots (Figure S1, Supplementary Materials). The presence of these sharp spikes reveals that some of these

contacts occurred at distances shorter than the van der Waals radii sum of the atoms sharing this contact. The pattern of the fingerprint plot for the N . . . H and C . . . H interactions indicated that the surface acts as both a hydrogen bond donor and hydrogen bond acceptor. On the other hand, the surface acts mainly as a hydrogen bond acceptor with respect to the Cl . . . H interactions. In contrast, the surface is the hydrogen bond donor for the most important O . . . H interactions.

Similarly, the Hirshfeld surfaces of **1** are shown in Figure 8, where the decomposition of the fingerprint plot revealed the importance of the H . . . H and O . . . H contacts in the molecular packing. A summary of these short interactions is given in Table 6.

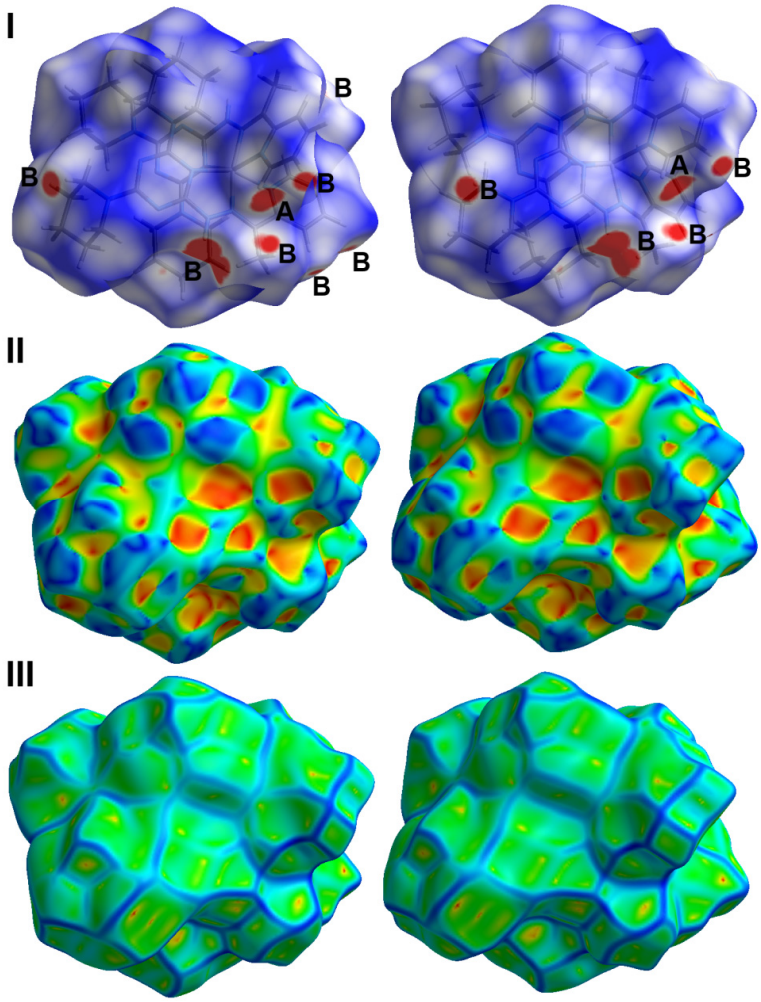

Figure 8. Hirshfeld surfaces: (**I**) d_{norm}, (**II**) shape index and (**III**) curvedness for **1**.

Table 6. The short intermolecular interactions in **1**.

Contact	Distance	Contact	Distance
H1 . . . H4B	1.677	O4 . . . H1	2.317
O1B . . . H14B	2.213	O3 . . . H4A	1.732
O2B . . . H3	1.928	O3B . . . H4B	1.711
O2B . . . H7A	2.208	O1 . . . H3A	2.507
O3 . . . H7A	2.315	O1B . . . H3A	2.456
O3 . . . H3	1.900	O1B . . . H4	2.560
O2 . . . H17B	2.540	O2 . . . H4	2.418
O4 . . . H7B	2.347	O1B . . . H2	2.338

The decomposition analysis of all contacts that occurred in the crystal structure of **1** is shown in Figure 9. The most dominant intermolecular interactions are H . . . H, O . . . H and C . . . H contacts. Their percentages are 56.4, 21.8 and 13.3%, respectively. Only the H . . . H and O . . . H interactions have the most significance in the molecular packing of **1**, as further revealed from their fingerprint plots shown in (Figure S2, Supplementary Materials).

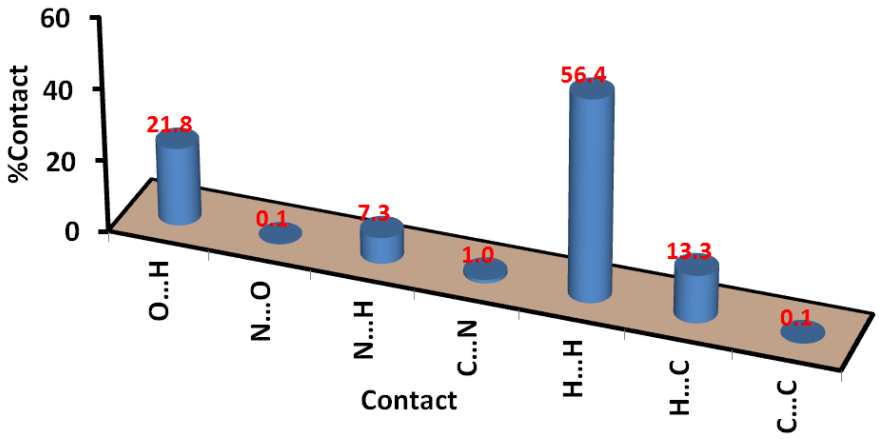

Figure 9. Intermolecular interactions in **1**.

2.4. Antimicrobial Evaluations

The results of the antimicrobial evaluations of the studied compounds against selected microbes (Table 7). It is clear that the free ligand has no activity against microbes except *B. subtilis*, where the inhibition zone diameter is only 10 mm while the MIC value is 1250 µg/mL. As a result, the free ligand has weak antimicrobial activity against the studied microbes.

Table 7. Antimicrobial activities of **DPPT** and its Ni(II) complexes [a].

Microbes	DPPT	1	2	Control
Fungi				
A. fumigatus	NA [b] (ND) [c]	20 (312)	18 (312)	17 (156) [d]
C. albicans	NA [b] (ND) [c]	21 (312)	19 (312)	20 (312) [d]
Gram-positive				
S. aureus	NA[b] (ND) [c]	7 (5000)	8 (2500)	24 (9.7) [e]
B. subtilis	10 (1250)	19 (312)	22 (78)	26 (4.8) [e]
Gram-negative				
E.coli	NA [b] (ND) [c]	NA[b] (ND) [c]	NA[b] (ND) [c]	30 (4.8) [e]
P.vulgaris	NA [b] (ND) [c]	NA[b] (ND) [c]	NA[b] (ND) [c]	25 (4.8) [e]

[a] Values outside and inside parentheses for inhibition zone diameter (mm) and MIC (µg/mL), respectively; [b] NA: No activity; [c] ND: Not determined; [d] Ketoconazole and [e] *Gentamycin*.

On the other hand, the studied Ni(II) complexes have interesting antimicrobial activity against Gram-positive bacteria and fungi while not active against Gram-negative bacteria. In the case of complex **1**, the inhibition zone diameters are determined to be 20 and 21 mm against the fungi *A. fumigatus* and *C. albicans* while 7 and 19 mm against the Gram-positive bacteria *S. aureus* and *B. subtilis*, respectively. The corresponding values for **2** are 18, 19, 8 and 22 mm. Hence, complex **2** has slightly better antifungal activity than **1**. In contrast, complex **1** has better antibacterial activity against the two Gram-positive bacteria than **2**. The results of the MIC are in accord with the inhibition zone diameters, where the MIC is only 78 µg/mL for complex **2** against *B. subtilis*. The Ni(II) chelates could affect the respiration of the microbial organisms, which inhibits their ability to produce their own proteins leading to their death [38], which could explain the interesting antimicrobial activity. On the other hand, the studied Ni(II) complexes have moderate

activity compared to antifungal (Ketoconazole) and antibacterial (*Gentamycin*) controls. It is clear that both Ni(II) complexes have similar antifungal activity against *C. albicans* compared to Ketoconazole, where all have MIC values of 312 μg/mL.

In our previous work, the antimicrobial activity of the Cu(II), Mn(II) and Ni(II) complexes with **DMPT** was reported [36,37]. It was found that all complexes except the [Mn(DMPT)Cl_2] complex have no antifungal activity. In contrast, the Mn(II) and Cu(II) complexes of **DMPT** showed interesting antimicrobial activity against both Gram-positive and Gram-negative bacteria, while the corresponding Ni(II) complex has less antibacterial potency. Interestingly, the studied Ni(II) complexes **1** and **2** have improved antifungal and antibacterial activities compared to the previously published metal(II) analogues of **DMPT**. As a result, the modification of the structure of the coordinated ligand by replacement of the morpholine ring with piperidine has a significant impact on the improvement of the antimicrobial activity.

3. Materials and Methods

3.1. Physical Measurements

All details regarding the instrumentations and chemicals are given in Supplementary Materials. FTIR and NMR spectra of **DPPT** are shown in Figures S3–S5 (Supplementary Materials).

3.2. Synthesis of DPPT Ligand [36,37]

The synthetic method for the ligand **DPPT** is similar to the previously reported method [36,37] in which refluxed in EtOH an equimolar of the 2-acetylpyridine and *s*-triazine-hydrazine derivative in the presence of catalytic amount of AcOH. The product obtained is white material (Scheme 1).

Ligand (DPPT): m.p: 188–190 °C; IR (KBr, cm^{-1}): 3279 $\nu_{(N-H)}$, 3059 $\nu_{(C-H)}$, 3003 $\nu_{(C-H)}$, 2937 $\nu_{(C-H)}$, 1597 $\nu_{(C=N)}$, 1514 $\nu_{(C=C)}$. ^{1}H NMR (400 MHz, CDl_3) δ 8.52 (d, *J* = 4.8 Hz, 1H), 8.23 (d, *J* = 8.0 Hz, 1H), 8.17 (broad-s, 1H NH), 7.66 (t, *J* = 7.7 Hz, 1H), 7.22–7.14 (m, 1H), 3.76 (t, *J* = 5.4 Hz, 8H), 2.38 (s, 3H), 1.60 (dq, *J* = 16.9, 5.5 Hz, 12H). ^{13}C NMR (101 MHz, CDl_3) δ 165.04, 164.70, 155.86, 148.34, 146.61, 136.31, 136.05, 123.24, 122.07, 120.96, 120.60, 44.26, 25.96, 24.99, 10.67.

3.3. Synthesis of Ni(II) Complexes

3.3.1. Synthesis of [Ni(DPPT)$_2$]$(NO_3)_2$*1.5H_2O (**1**)

$Ni(NO_3)_2$.6H_2O (43.6 mg, 0.15 mmol) in 8 mL ethanol was mixed with 8 mL ethanolic solution of organic ligand **DPPT** (114.0 mg, 0.3 mmol). The resulting clear green solution was allowed to evaporate slowly and crystallize at room temperature. After one week, green crystals of complex **1** were collected by filtration.

Complex **1**, Anal. Calc. $C_{80}H_{118}N_{36}Ni_2O_{15}$: C, 49.49; H, 6.13; N, 25.97; Ni, 6.05%. Found: C, 49.31; H, 6.05; N, 25.80; Ni, 5.95%.

3.3.2. Synthesis of [Ni(DPPT)(NO_3)Cl].EtOH (**2**)

Equimolar amounts of 8 mL ethanolic solution of $Ni(NO_3)_2$*6H_2O (43.7 mg, 0.15 mmol) and $NiCl_2$*6H_2O (35.7 mg, 0.15 mmol) were added to 8 mL ethanolic solution of organic ligand **DPPT** (114.0 mg, 0.3 mmol). The clear mixture was left at room temperature. After 10 days, green crystals of complex **2** were collected by filtration.

Complex **2**, Anal. Calc. $C_{22}H_{34}ClN_9NiO_4$: C, 45.35; H, 5.88; N, 21.63; Ni, 10.07%. Found: C, 45.19; H, 5.79; N, 21.47; Ni, 9.96%. IR (KBr, cm^{-1}): 3456 $\nu_{(O-H)}$, 3230 $\nu_{(N-H)}$, 3132 $\nu_{(N-H)}$, 3072 $\nu_{(C-H)}$, 3007 $\nu_{(C-H)}$, 2933 $\nu_{(C-H)}$, 1603 $\nu_{(C=N)}$, 1569 $\nu_{(C=N)}$, 1497 $\nu_{(C=C)}$, 1381 ν(N–O).

3.4. Crystal Structure Determination

Details of solving the X-ray structures of **1** and **2** are given in Supplementary Materials [39–43]. The crystallographic details are summarized in Table 8.

Table 8. Crystal Data.

	1	**2**
CCDC no.	2264028	2264029
empirical formula	$C_{80}H_{118}N_{36}Ni_2O_{15}$	$C_{22}H_{34}ClN_9NiO_4$
fw	1941.52	582.74
temp (K)	170(2)	170(2)
λ (Å)	0.71073	0.71073 Å
cryst syst	Monoclinic	Triclinic
space group	C2/c	P $\bar{1}$
a (Å)	22.5323(7)	8.8007(2)
b (Å)	13.1439(2)	12.2506(2)
c (Å)	15.9387(5)	12.5275(2)
α (deg)		81.2940(10)
β (deg)	106.8490(10)	82.3740(10)
γ (deg)		74.8340(10)
V (Å^3)	4517.8(2)	1282.43(4)
Z	2	2
ρ_{calc} (Mg/m^3)	1.427	1.509
μ(Mo Kα) (mm^{-1})	0.501	0.909
No. reflns.	25970	27302
Completeness to theta = 25.242°	99.8%	99.5%
Unique reflns.	4271	7451
GOOF (F^2)	1.087	1.070
R_{int}	0.0502	0.0284
R_1 [a] ($I \geq 2\sigma$)	0.0535	0.0382
wR_2 [b] ($I \geq 2\sigma$)	0.1096	0.0807

[a] $R_1 = \Sigma||F_o| - |F_c||/\Sigma|F_o|$. [b] $wR_2 = [\Sigma[w(F_o^2 - F_c^2)^2]/\Sigma[w(F_o^2)^2]]^{1/2}$.

3.5. Hirshfeld Analysis

The Crystal Explorer Ver. 3.1 program [44] was used to perform this analysis.

3.6. Antimicrobial Assay

The methods used for determining antibacterial activity are mentioned in Method S1 (Supplementary Materials) [45].

4. Conclusions

The supramolecular structure of the newly synthesized complexes, $[Ni(DPPT)_2](NO_3)_2$*$1.5H_2O$ (**1**) and $[Ni(DPPT)(NO_3)Cl]$.EtOH (**2**), was described based on X-ray single-crystal structural and Hirshfeld analyses. The intermolecular contacts H . . . H and O . . . H in **1** and Cl . . . H, O . . . H, N . . . H, H . . . H, C . . . H and C . . . C in **2** are the most important to crystal stability. Both complexes have distorted octahedral coordination environments around the Ni(II) ion, where the **DPPT** ligand is a tridentate chelate. The coordination environment of Ni(II) in **2** is completed by one bidentate nitrate and one chloride ion. Complexes **1** and **2** have similar antifungal activity against *C. albicans* compared to Ketoconazole. Additionally, both Ni(II) complexes are better antibacterial and antifungal agents than the free ligand. In comparison with our previous work, the replacement of the morpholine ring by piperidine moiety at the *s*-triazine core has a significant impact on the improvement of the antimicrobial activity.

Supplementary Materials: The following supporting information can be downloaded at: https://www.mdpi.com/article/10.3390/inorganics11060253/s1. Crystal structure determination; Physical measurements; Crystal structure determination; Method S1. Evaluation of antimicrobial activity; Figure S1. Fingerprint plots for the important interactions in **2**; Figure S2. Fingerprint plots for the important interactions in **1**; Figure S3 FTIR spectra of DPPT; Figure S4 ^{1}H NMR spectra of DPPT; Figure S5 ^{13}C NMR spectra of DPPT.

Author Contributions: Conceptualization, M.A.M.A.-Y. and S.M.S.; formal analysis, E.M.F., M.M.S. and M.H.; investigation, E.M.F.; methodology, E.M.F. and A.B.; software, M.H. and S.M.S.; supervision, M.A.M.A.-Y., A.B. and S.M.S.; validation, A.E.-F. and A.B.; visualization, A.E.-F.; writing—original draft, S.M.S.; writing—review and editing, M.A.M.A.-Y., A.E.-F. and A.B. All authors have read and agreed to the published version of the manuscript.

Funding: The authors would like to extend their sincere appreciation to the Researchers Supporting Project (RSP2023R64), King Saud University, Riyadh, Saudi Arabia.

Data Availability Statement: Not applicable.

Acknowledgments: The authors would like to extend their sincere appreciation to the Researchers Supporting Project (RSP2023R64), King Saud University, Riyadh, Saudi Arabia.

Conflicts of Interest: The authors declare no conflict of interest.

References

1. Raithby, G.L.; De Leon, J.; Karra-Aly, A.; Osman, A.A.; Boyd, C.L.; Saini, G.K.; Sehra, J.S.; Ikenyei, U.C. An Innovative Approach to Improve Canada's Infectious Disease Pandemic Rapid Response in Marginalized Communities. *Glob. Health Annu. Rev.* **2020**, *1*, 3.
2. World Health Organization. Global Antimicrobial Resistance and Use Surveillance System (GLASS) Report: 2021; World Health Organization: 2021. Available online: https://www.who.int/publications/i/item/9789240027336 (accessed on 22 May 2023).
3. Guo, Z.; Sadler, P.J. Medicinal inorganic chemistry. *Adv. Inorg. Chem.* **1999**, *49*, 183–306.
4. Barrios, A.M.; Cohen, S.M.; Lim, M.H. Medicinal inorganic chemistry: A web themed issue. *Chem. Commun.* **2013**, *49*, 5910–5911. [CrossRef]
5. Mjos, K.D.; Orvig, C. Metallodrugs in medicinal inorganic chemistry. *Chem. Rev.* **2014**, *114*, 4540–4563. [CrossRef]
6. El-Sherif, A.A. Synthesis, spectroscopic characterization and biological activity on newly synthesized copper (II) and nickel (II) complexes incorporating bidentate oxygen–nitrogen hydrazone ligands. *Inorg. Chim. Acta.* **2009**, *362*, 4991–5000. [CrossRef]
7. Singh, K.; Kumar, Y.; Puri, P.; Kumar, M.; Sharma, C. Cobalt, nickel, copper and zinc complexes with 1, 3-diphenyl-1H-pyrazole-4-carboxaldehyde Schiff bases: Antimicrobial, spectroscopic, thermal and fluorescence studies. *Eur. J. Med. Chem.* **2012**, *52*, 313–321. [CrossRef]
8. Tharmaraj, P.; Kodimunthiri, D.; Sheela, C.D.; Shanmuga Priya, C.S. Synthesis, spectral characterization, and antimicrobial activity of copper (II), cobalt (II), and nickel (II) complexes of 3-formylchromoniminopropylsilatrane. *J. Coord. Chem.* **2009**, *62*, 2220–2228. [CrossRef]
9. Raman, N.; Mutijuraj, V.; Rovichandran, S.; Kulandaisamy, A. Electrochemical Behavior of Cu (II), Co (II), Ni (II) and Zn (II) complexes derived from acetylacetone and p-anisidine and their antimicrobial activity. *Proc. Indian Acad. Sci.* **2003**, *115*, 161–167. [CrossRef]
10. Chohan, Z.H.; Farooq, M.A. Synthesis, characterization, ligational and biological properties of some acylhydrazine derived furanyl and thienyl Schiff bases with Co(II), Cu(II), Ni(II), and Zn(II) metal ions. *Synth. React. Inorg. Met. Org. Chem.* **2001**, *31*, 1853–1871. [CrossRef]
11. Jouad, E.M.; Larcher, G.; Allain, M.; Riou, A.; Bouet, G.M.; Khan, M.A.; Do Thanh, X. Synthesis, structure and biological activity of nickel (II) complexes of 5-methyl 2-furfural thiosemicarbazone. *J. Inorg. Biochem.* **2001**, *86*, 565–571. [CrossRef] [PubMed]
12. Dixon, N.E.; Gazzola, C.; Blakeley, R.L.; Zerner, B. Jack bean urease (EC 3.5. 1.5). Metalloenzyme. Simple biological role for nickel. *J. Am. Chem. Soc.* **1975**, *97*, 4131–4133. [CrossRef]
13. Raj, P.; Singh, A.; Singh, A.; Singh, N. Syntheses and photophysical properties of Schiff base Ni (II) complexes: Application for sustainable antibacterial activity and cytotoxicity. *ACS Sustain. Chem. Eng.* **2017**, *5*, 6070–6080. [CrossRef]
14. Kasuga, N.C.; Sekino, K.; Koumo, C.; Shimada, N.; Ishikawa, M.; Nomiya, K. Synthesis, structural characterization and antimicrobial activities of 4-and 6-coordinate nickel (II) complexes with three thiosemicarbazones and semicarbazone ligands. *J. Inorg. Biochem.* **2001**, *84*, 55–65. [CrossRef]
15. Kurtaran, R.; Yıldırım, L.T.; Azaz, A.D.; Namli, H.; Atakol, O. Synthesis, characterization, crystal structure and biological activity of a novel heterotetranuclear complex: [NiLPb (SCN) 2 (DMF)(H2O)] 2, bis-{[μ-N, N′-bis (salicylidene)-1, 3-propanediaminato-aqua-nickel(II)](thiocyanato)(μ-thiocyanato)(μ-N,N′ dimethylformamide) lead (II)}. *J. Inorg. Biochem.* **2005**, *99*, 1937–1944.
16. Kasuga, N.C.; Ohashi, A.; Koumo, C.; Uesugi, J.; Oda, M.; Nomiya, K. Synthesis, Structural Characterization, and Biological Activity of Two Different Nickel (II) Complexes Derived from N′-[1-(2-pyridyl) ethylidene] morpholine-4-carbothiohydrazide. *Chem. Lett.* **1997**, *26*, 609–610. [CrossRef]
17. Oladipo, S.D.; Omondi, B.; Mocktar, C. Synthesis and structural studies of nickel (II)-and copper (II)-N, N′-diarylformamidine dithiocarbamate complexes as antimicrobial and antioxidant agents. *Polyhedron* **2019**, *170*, 712–722. [CrossRef]
18. Alexiou, M.; Tsivikas, I.; Dendrinou-Samara, C.; Pantazaki, A.A.; Trikalitis, P.; Lalioti, N.; Kyriakidis, D.A.; Kessissoglou, D.P. High nuclearity nickel compounds with three, four or five metal atoms showing antibacterial activity. *J. Inorg. Biochem.* **2003**, *93*, 256–264. [CrossRef]

19. Skyrianou, K.C.; Efthimiadou, E.K.; Psycharis, V.; Terzis, A.; Kessissoglou, D.P.; Psomas, G. Nickel–quinolones interaction. Part 1–Nickel (II) complexes with the antibacterial drug sparfloxacin: Structure and biological properties. *J. Inorg. Biochem.* **2009**, *103*, 1617–1625. [CrossRef]
20. Kerru, N.; Gummidi, L.; Maddila, S.; Gangu, K.K.; Jonnalagadda, S.B. A review on recent advances in nitrogen-containing molecules and their biological applications. *Molecules* **2020**, *25*, 1909. [CrossRef]
21. Gordon, E.M.; Barrett, R.W.; Dower, W.J.; Fodor, S.P.A.; Gallop, M.A. Applications of combinatorial technologies to drug discovery, combinatorial organic synthesis, library screening strategies, and future directions. *J. Med. Chem.* **1994**, *37*, 1385–1401. [CrossRef]
22. Zhang, B.; Studer, A. Recent advances in the synthesis of nitrogen heterocycles via radical cascade reactions using isonitriles as radical acceptors. *Chem. Soc. Rev.* **2015**, *44*, 3505–3521. [CrossRef]
23. Walsh, C.T. Nature loves nitrogen heterocycles. *Tetrahedron Lett.* **2015**, *56*, 3075–3081. [CrossRef]
24. Angelusiu, M.V.; Barbuceanu, S.F.; Draghici, C.; Almajan, G.L. New Cu (II), Co (II), Ni (II) complexes with aroyl-hydrazone based ligand. Synthesis, spectroscopic characterization and in vitro antibacterial evaluation. *Eur. J. Med. Chem.* **2010**, *45*, 2055–2062. [CrossRef]
25. Wang, Q.; Yang, Z.Y.; Qi, G.F.; Qin, D.D. Crystal structures, DNA-binding studies and antioxidant activities of the Ln(III) complexes with 7-methoxychromone-3-carbaldehyde-isonicotinoyl hydrazone. *BioMetals* **2009**, *22*, 927–940. [CrossRef]
26. Aslan, H.G.; Özcan, S.; Karacan, N. Synthesis, characterization and antimicrobial activity of salicylaldehyde benzenesulfonylhydrazone (Hsalbsmh) and its Nickel (II), Palladium (II), Platinum (II), Copper (II), Cobalt (II) complexes. *Inorg. Chem. Commun.* **2011**, *14*, 1550–1553. [CrossRef]
27. Naskar, S.; Naskar, S.; Butcher, R.J.; Chattopadhyay, S.K. Synthesis, X-ray crystal structures and spectroscopic properties of two Ni (II) complexes of pyridoxal Schiff's bases with diamines: Importance of steric factor in stabilization of water helices in the lattices of metal complex. *Inorg. Chim. Acta.* **2010**, *363*, 404–411. [CrossRef]
28. Xu, Z.H.; Zhang, X.W.; Zhang, W.Q.; Gao, Y.H.; Zeng, Z.Z. Synthesis, characterization, DNA interaction and antibacterial activities of two tetranuclear cobalt (II) and nickel (II) complexes with salicylaldehyde 2-phenylquinoline-4-carboylhydrazone. *Inorg. Chem. Commun.* **2011**, *14*, 1569–1573. [CrossRef]
29. Kratz, F.; Beyer, U.; Roth, T.; Tarasova, N.; Collery, P.; Lechenault, F.; Cazabat, A.; Schumacher, P.; Unger, C.; Falken, U. Transferrin conjugates of doxorubicin: Synthesis, characterization, cellular uptake, and in vitro efficacy. *J. Pharm. Sci.* **1998**, *87*, 338–346. [CrossRef]
30. Soliman, S.M.; El-Faham, A.; Albering, J.H. Synthesis, X-ray crystal structure and DFT studies of two octahedral cobalt(II) complexes with N,N,N-tridentate triazine-type ligand. *J. Coord. Chem.* **2017**, *70*, 2261–2279. [CrossRef]
31. Zerkowski, J.A.; Seto, C.T.; Whitesides, G.M. Solid-state structures of rosette and crinkled tape motifs derived from the cyanuric acid melamine lattice. *J. Am. Chem. Soc.* **1992**, *114*, 5473–5475. [CrossRef]
32. Demeshko, S.; Dechert, S.; Meyer, F. Anion-π Interactions in a Carousel Copper(II)-Triazine Complex. *J. Am. Chem. Soc.* **2004**, *126*, 4508–4509. [CrossRef] [PubMed]
33. Ramírez, J.; Stadler, A.-M.; Brelot, L.; Lehn, J.-M. Coordinative, conformational and motional behaviour of triazine-based ligand strands on binding of Pb(II) cations. *Tetrahedron* **2008**, *64*, 8402–8410. [CrossRef]
34. Vilaivan, T.; Saesaengseerung, N.; Jarprung, D.; Kamchonwongpaisan, S.; Sirawaraporn, W.; Yuthavong, Y. Synthesis of Solution-Phase Combinatorial Library of 4,6-Diamino-1,2-dihydro-1,3,5-triazine and Identification of New Leads Against A16V+S108T Mutant Dihydrofolate Reductase of Plasmodium falciparum. *Bioorgan. Med. Chem.* **2002**, *11*, 217–224. [CrossRef]
35. Osman, S.M.; Khattab, S.; Aly, E.-S.A.; Kenawy, E.-R.; El-Faham, A. 1,3,5-Triazine-based polymer: Synthesis, characterization and application for immobilization of silver nanoparticles. *J. Polym. Res.* **2017**, *24*, 231. [CrossRef]
36. Fathalla, E.M.; Abu-Youssef, M.A.M.; Sharaf, M.M.; El-Faham, A.; Barakat, A.; Badr, A.M.A.; Soliman, S.M.; Slawin, A.M.Z.; Woollins, J.D. Synthesis, Characterizations, Antitumor and Antimicrobial Evaluations of Novel Mn(II) and Cu(II) Complexes with NNN-tridentate s-Triazine-Schiff base Ligand. *Inorg. Chim. Acta* **2023**, *555*, 121586. [CrossRef]
37. Fathalla, E.M.; Abu-Youssef, M.A.M.; Sharaf, M.M.; El-Faham, A.; Barakat, A.; Haukka, M.; Soliman, S.M. Synthesis, X-ray Structure of Two Hexa-Coordinated Ni(II) Complexes with *s*-Triazine Hydrazine Schiff Base Ligand. *Inorganics* **2023**, *11*, 222. [CrossRef]
38. Sherif, O.E.; Abdel-Kader, N.S. DFT calculations, spectroscopic studies, thermal analysis and biological activity of supramolecular Schiff base complexes. *Arab. J. Chem.* **2018**, *11*, 700–713. [CrossRef]
39. Otwinowski, Z.; Minor, W. Processing of X-ray Diffraction Data Collected in Oscillation Mode. *Methods Enzymol.* **1997**, *276*, 307–326.
40. Sheldrick, G.M. Shelxt–integrated space-group and crystal-structure determination. *Acta Cryst.* **2015**, *A71*, 3–8. [CrossRef] [PubMed]
41. Sheldrick, G.M. *SADABS—Bruker Nonius Scaling and Absorption Correction*; Bruker AXS, Inc.: Madison, WI, USA, 2012.
42. Sheldrick, G.M. Crystal structure refinement with SHELXL. *Acta Cryst.* **2015**, *C71*, 3–8.
43. Hübschle, C.B.; Sheldrick, G.M.; Dittrich, B. *ShelXle*: A Qt graphical user interface for *SHELXL*. *J. Appl. Crystallogr.* **2011**, *44*, 1281–1284. [CrossRef] [PubMed]

44. Spackman, M.A.; Jayatilaka, D. Hirshfeld Surface Analysis. *CrystEngComm* **2009**, *11*, 19–32. [CrossRef]
45. Lu, P.-L.; Liu, Y.-C.; Toh, H.-S.; Lee, Y.-L.; Liu, Y.-M.; Ho, C.-M.; Huang, C.-C.; Liu, C.-E.; Ko, W.-C.; Wang, J.-H. Epidemiology and antimicrobial susceptibility profiles of Gram-negative bacteria causing urinary tract infections in the Asia-Pacific region: 2009–2010 results from the Study for Monitoring Antimicrobial Resistance Trends (SMART). *Int. J. Antimicrob. Agents* **2012**, *40*, S37–S43. [CrossRef] [PubMed]